Journal of Solid State Chemistry **158,** 208–217 (2001)
doi:10.1006/jssc.2001.9094, available online at http://www.idealibrary.com on IDEAL®

Spin State Transition in $LaCoO_3$ with Temperature or Strontium Doping as Seen by XAS

O. Toulemonde,[1] N. N'Guyen, and F. Studer

Laboratoire CRISMAT, CNRS–UMR 6508, ISMRA, Bovlevard du Mal Juin, 14050 Caen Cedex, France

and

A. Traverse

Laboratoire Lure, bat 209D, Centre Universtaire Paris—Sud 91405 Orsay Cedex, France

Received August 10, 2000; in revised form January 3, 2001; accepted January 19, 2001; published online April 5, 2001

An X-ray absorption spectroscopy study of the polycrystalline $La_{1-x}Sr_xCoO_3$ ($x = 0$, 0.25, 0.5) series at O K-edge was performed above and below the various magnetic transition temperatures. A crystal field analysis is proposed to explain the observed fine structure changes. Temperature-dependent O K-edge of $LaCoO_3$ shows evidence of smooth and continuous spin transition of Co^{3+} from low to intermediate spin states. This result is confirmed by cobalt K-edge measurements. Upon strontium doping, O K-edges of the $La_{1-x}Sr_xCoO_3$ ($x = 0$, 0.25, 0.5) series suggested a mixed (LS–IS) Co^{3+}/IS Co^{4+} cobalt ion configuration. The fundamental mechanism governing the magnetotransport properties shown by the compounds is then discussed.

I. INTRODUCTION

Since the discovery of colossal magnetoresistance (CMR) in manganese oxides, which depends first on the nature and on the substitution rate of rare-earth or alkaline-earth elements on the perovskite *A* site (1) and second, in the case of charge ordered compounds, on the doping rate by a transition metal on the perovskite *B* site (2), magnetoresistance effects have been observed either in transition-metal perovskites like cobaltites $La_{1-x}Sr_xCoO_3$ (3), or in double-perovskite like $LnNi_{0.3}Co_{0.7}O_3$ (4) and Sr_2FeMoO_6 (5).

In the case of $La_{1-x}Sr_xCoO_3$ solid solution, the parent compound $LaCoO_3$ exhibits a semiconducting behavior below room temperature. Its ground state is known to be nonmagnetic Co^{3+} ($S = 0$, t_{2g}^6) at zero (6), which is in agreement with LDA + U band structure calculations performed by Korotin *et al.* (7) Then, with increasing temperature, the low spin state changes into higher spin configurations, which is still controversial. Some authors (7–11) claimed that a change from a low spin to an intermediate spin configuration ($S = 1$, $t_{2g}^5 e_g^1$) should occur while others (6, 12, 13) suggest the formation of a mixed-spin ($S = 0$, t_{2g}^6/$S = 2$, $t_{2g}^4 e_g^2$). Then, at higher temperature, $LaCoO_3$ becomes metallic (8, 14).

Substitution of Sr^{2+} for La^{3+} in $La_{1-x}Sr_xCoO_3$ oxidizes the cobalt assuming a fixed oxygen stoichiometry. Variations in the magnetic and transport properties with strontium doping have been observed previously (3). Both $La_{1-x}Sr_xCoO_3$ ($x = 0.25$; 0.5) compounds exhibit a paramagnetic to ferromagnetic transition. But, whereas the $La_{0.75}Sr_{0.25}CoO_3$ sample presents a controversial reentrants semiconducting behavior at low temperature, after a semiconducting/metal-like transition which occurs at the paramagnetic/ferromagnetic transition (3, 13), the $La_{0.5}Sr_{0.5}CoO_3$ sample exhibits a metal-like behavior in the whole temperature range.

In this paper, we present an X-ray absorption spectroscopy study of the $La_{1-x}Sr_xCoO_3$ ($x = 0$, 0.25, 0.5) compounds below room temperature in order to investigate the cobalt spin transition. It is believed to occur at the first magnetic transition around 100 K in the case of $LaCoO_3$ and it should occur upon strontium doping as suggested by the neutron studies of Loucas *et al.* (11) and Caciuffo *et al.* (15). Oxygen K- and cobalt K-edges were then recorded depending on doping amount and temperature.

II. EXPERIMENTAL

$La_{1-x}Sr_xCoO_3$ ($x = 0, 0.25, 0.5$) samples were prepared in the form of sintered pellets following a classical method of

[1] To whom correspondence should be addressed. Present address: Faculty of Mathematics, Computer Science, Physics, and Astronomy, University of Amsterdam, Valckenierstraat 65, NL 1018 XE Amsterdam, Netherlands.

0022-4596/01 $35.00

solid state chemistry. Thorough mixtures of $SrCO_3$, CoO_{1-x}, and La_2O_3 were first heated in air at 800°C for 12 h. The samples were then pressed into pellets and sintered first at 1000°C and then at 1100°C for 24 h in air. X-ray powder diffraction measurement showed single-phase patterns. The oxygen content was determined by chemical titration. The $La_{1-x}Sr_xCoO_{3-\delta}$ $(x = 0, 0.25, 0.5)$ samples can be considered stoichiometric with $\delta < 0.03$. Furthermore, from the amount used of $SrCO_3$ and CoO_{1-x} as starting materials, the cationic stoichiometries could be slightly different from those expected, but the comparison of our measured transport and magnetization properties with previous work allowed us to consider the cation amounts as stoichiometric.

Magnetization curves M(T) were established with a vibrating sample magnetometer. Samples were first zero-field cooled to 5 K before the magnetic field was applied. Resistance measurements were performed with the four-probe technique on sintered bars with $2 \times 2 \times 10\ mm^3$ dimensions. Both magnetization and transport measurements were carried out under warming.

X-ray absorption studies were performed systematically on the samples previously studied for their transport and magnetic properties. X-ray absorption spectra at O K-edges were recorded using light at the Dragon beamline (U4B) of the NSLS (BNL, USA) in the fluorescence detection mode. The base pressure in the spectrometer chamber was better than 10^{-9} mbar before cooling. The samples were scraped *in situ* just before measurements. The energy resolution using a slit width of 10 μm was estimated to be 0.11 eV at O K-edge. A standard procedure was adopted to remove the background contribution from the pre-edge baseline of the spectra. Then the normalization for the various studied compounds was obtained by equalizing the integrated area under the high energy part of the spectra, the covalent spectra, between 532 and 550 eV. All spectra at O K-edge were calibrated with respect to the absorption energy of the O1s first peak on a NiO single crystal used as a standard.

The temperature dependence of the X-ray absorption spectra at Co K-edges were recorded in a classical transmission mode at the EXAFS I station (channel cut monochromator) using the synchrotron radiation of the DCI storage ring of LURE (Orsay, France). The energy resolution at Co K-edge is estimated to 1.3 eV, whereas the reproducibility of the monochromator position is better than 0.3 eV. A cobalt metal K-edge was run simultaneously with all the measurements for precise energy calibration. The relative energies between various spectra were established by careful comparison of the derivative metal transition spectra. The normalization procedure used throughout this work was the following: after subtraction of the background on the EXAFS spectrum, a point located at an energy of 800 eV from the edge, where no more EXAFS oscillations were still observable, was set to unity. Then, a point at an energy between 50 and 100 eV from the edge and intensity set equal to one is labeled on the EXAFS spectrum. After subtraction of the background on the XANES spectrum, the height is normalized by setting to unity the point with the same energy as the one labeled on the EXAFS spectrum as defined previously.

III. RESULTS AND DISCUSSION

III.1. Physical Properties

a. Magnetization measurements. Figure 1 shows the temperature dependence of the magnetization for the parent compound $LaCoO_3$ recorded under 1.45 T. The result essentially agrees with previous data (6, 14, 16). One could observe upon warming a magnetic transition at 110 K. First, the increase of the susceptibility value with temperature increase was interpreted by the previous authors as a spin transition from Co^{3+} low spin ($S = 0$, t_{2g}^6) to higher spin state driven by thermal activation (6). It should be noticed that no antiferromagnetic long-range order has been found by neutron scattering experiment (17). Then, antiferromagnetic long-range order could not be taken into account to explain the magnetic transition. As it will be discussed later, O–K absorption edge was performed in order to provide useful informations on the spin-state transition, which is believed to drive the magnetic transition.

Figures 2 and 3 show, respectively, the temperature dependence of the magnetization of the strontium-doped compounds $La_{1-x}Sr_xCoO_3$ for $x = 0.25$ and 0.5, respectively, recorded under 100 Gauss and 1.45 T. Upon decrease of the temperature, the compounds exhibit a transition from a paramagnetic to a ferromagnetic state at $T_c = 205$ K for $x = 0.25$ and $T_c = 250$ K for $x = 0.5$. For a weak applied

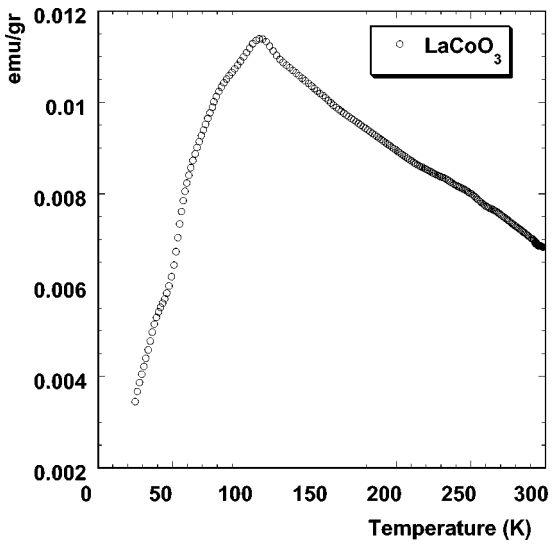

FIG. 1. Thermal variation of the magnetization of the sample $LaCoO_3$ under 1.45 T.

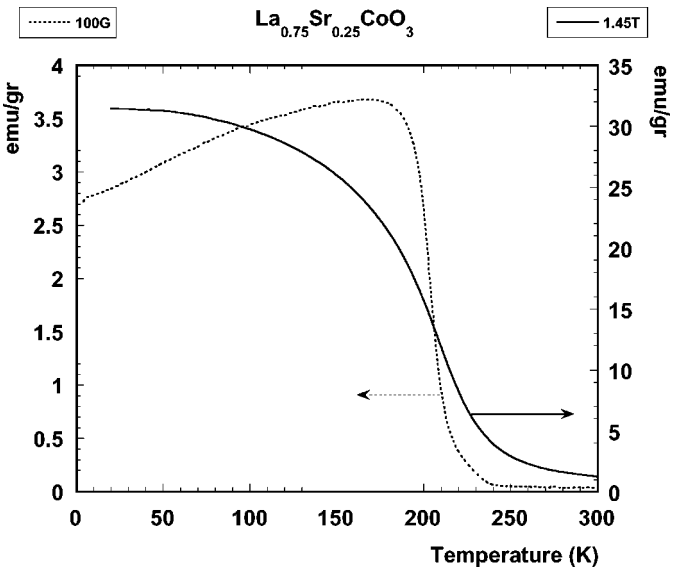

FIG. 2. Thermal variation of the magnetization of the sample $La_{0.75}Sr_{0.25}CoO_3$ under 1.45 and 0.01 T.

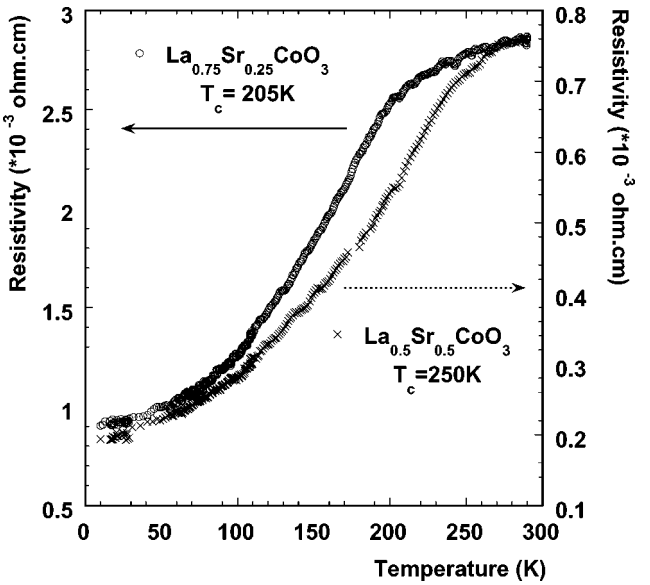

FIG. 4. Thermal variation of the resistance of the samples $La_{0.5}Sr_{0.5}CoO_3$ and $La_{0.75}Sr_{0.25}CoO_3$.

magnetic field (0.01 T), both compounds exhibit a smooth reduction of magnetization below the transition temperature T_c. Conversely, for a large applied magnetic field (1.45 T), the magnetization turns to saturation at low temperature but the transition width at the ferromagnetic ordering increases drastically with the applied magnetic field. Such a result is usually observed in the CMR rare-earth manganites under the same measurement conditions (18) and is likely due to the distribution of magnetic moments induced by a variable spread in energy of magnetic polarons (15, 19). Hence, the difference in the thermal variations of magnetization under different applied magnetic fields indicates that no simple ferromagnetic long-range ordering is achieved in the studied strontium-doped cobaltites, and that a cluster glass ferromagnetic state is more likely to be obtained.

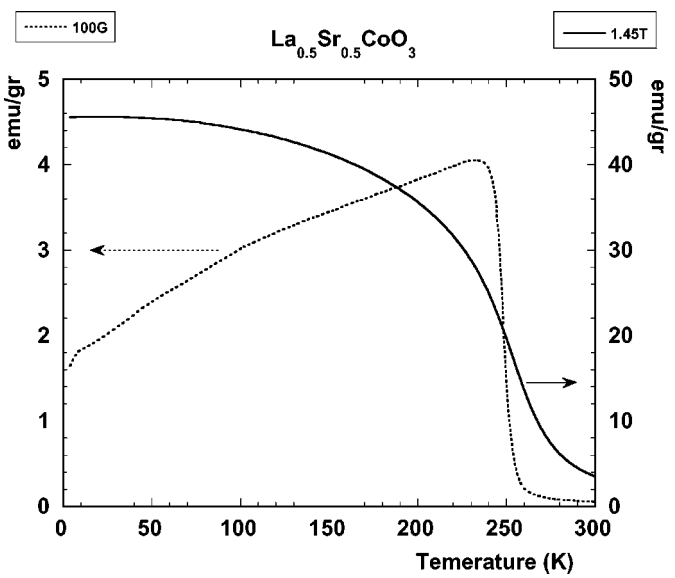

FIG. 3. Thermal variation of the magnetization of the sample $La_{0.5}Sr_{0.5}CoO_3$ under 1.45 and 0.01 T.

b. Transport properties. Figure 4 shows the resistivity measurements of the two strontium-doped compounds. In this figure, the symbol sizes are larger than the experimental errors. It should be noted that for $x = 0.25$ resistivity is higher than for $x = 0.5$, which is in agreement with the increase of the doping hole density and previous measurements (20). Futhermore, contrary to what has been observed in manganese oxides, no spontaneous transition from insulating to metal-like state behavior can be observed; the resistivity of strontium-doped cobaltites gradually decreases upon the decrease in temperature, whereas for usual metal behavior, the resistivity versus temperature should be linear. However, this observed behavior originates from double exchange arising from the Co^{3+}–O^{2-}–Co^{4+} interactions that allows one to correlate ferromagnetic interactions with metal-like behavior (21); the resistivity drops gradually as soon as the short-range ferromagnetic ordering occurs. It has already been shown by Yamaguchi *et al.* (3) that the magnitude of the magnetoresistance is proportional to the square of the magnetization.

III.2. Oxygen and Cobalt K-Edges Measurements in $LaCoO_3$

Figure 5a shows the temperature dependence of the O–K edge of $LaCoO_3$. The spectra could be divided in different

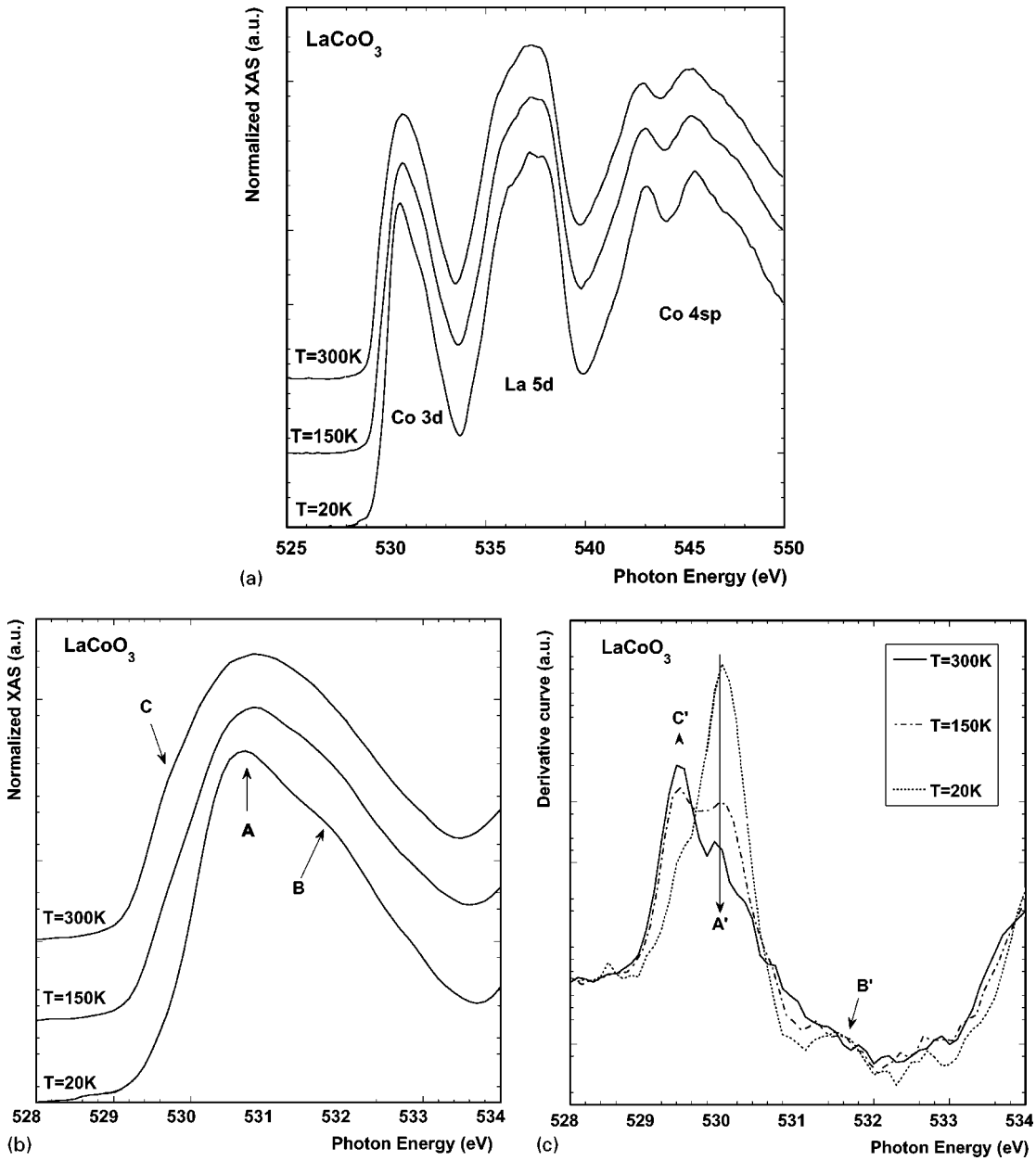

FIG. 5. Temperature dependence at $T = 20$, 150, and 300 K for $LaCoO_3$: (a) O K-edge; (b) O K-edge prepeak; (c) O K-edge derivative curve.

energy domains corresponding to various excitations from O 1*s* core level. More precisely, the first energy range (between 528 and 533.5 eV) corresponds to transitions which occur from O 1*s* core level to hybridized states between Co 3*d* and O 2*p* subbands. The next energy range (between 533.5 and 540.5 eV) corresponds to hybridization between mixed La 5*d*/Sr 4*s* and O 2*p* subbands, and, the highest energy range (between 540.5 and 550 eV), to hybridization between mixed Co 4*sp* and O 2*p* subbands (22).

Figures 5b and 5c show the O–K edge prepeak temperature dependence and the corresponding derivative curve of this O–K edge prepeak, respectively. At $T = 20$ K, the O–K edge prepeak shows a double peak structure (shoulders A and B) at 530.7 and 531.7 eV. With an increase in temperature, a continuous change in the O K-edge prepeak is observed, which is better evidenced on the derivative curve. Furthermore, the prepeak's width becomes larger at high temperature, whereas no significant growth in intensity is observed. Both static (lattice expansion) and dynamic (increased lattice vibration) structural modifications are candidates to explain those effects. The important thing is that new electronic states near the Fermi level must be considered to account for the observed changes in the O K-edges upon increasing temperature.

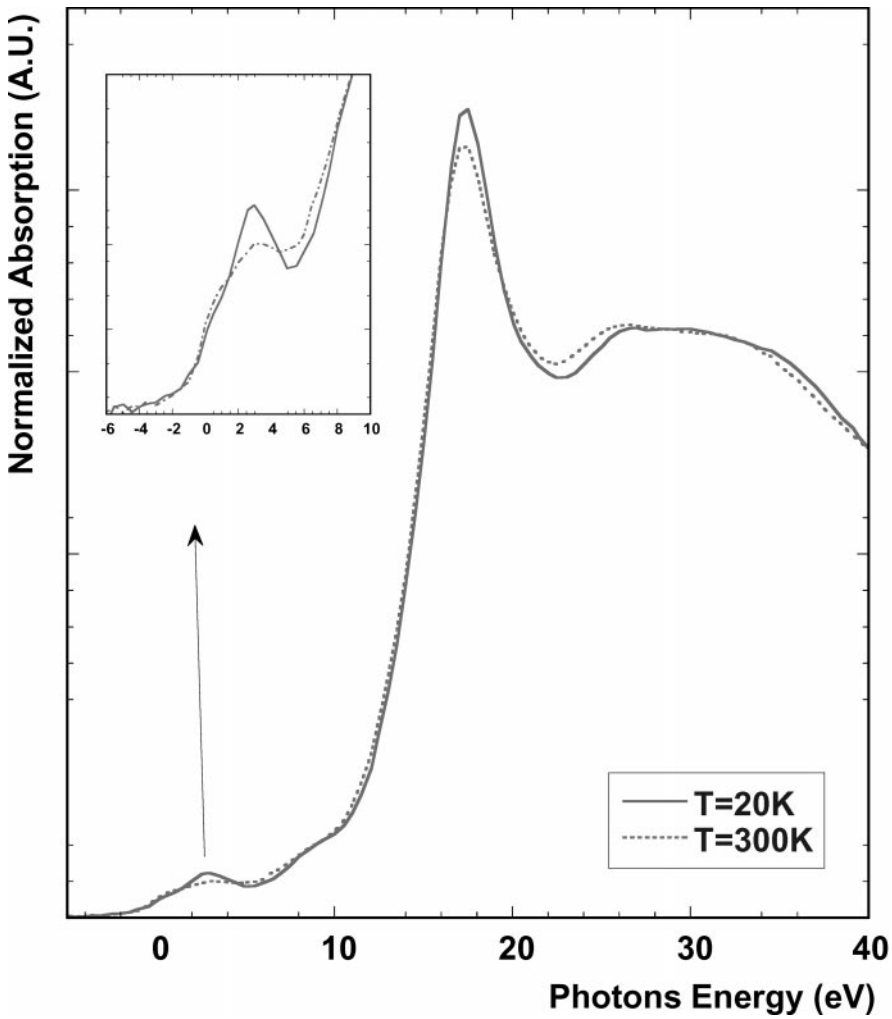

FIG. 6. Co K-edge temperature dependence at $T = 20$ and 300 K for $LaCoO_3$; (inset) pre-edge region.

On the cobalt K-edge temperature dependence (Fig. 6), principal modifications to the spectra are changes in intensity of the main line and in the shape of the pre-edge region, which is shown in detail in the inset. The main line is associated to dipolar transitions from Co 1*s* to 4*p* states, but the small pre-edge structure is associated to quadrupolar transitions from Co 1*s* to 3*d* states, then to states given by hybridization of the Co 3*d* band with the oxygen 2*p* band. Both a decrease of main line intensity and an increase of spectral weight of the pre-edge feature (we integrated the pre-edge intensity from -4 to 10 eV) when the temperature is increased are interpreted as Co(4*p*)–O(2*p*) and Co(3*d*)–O(2*p*) hybridization increasing, respectively (23). Note that the pre-edge fine structure at room temperature is more diffuse than at low temperature and that it is similar to previous Co K-edge room temperature measurements (24).

Considering that neutron diffraction temperature-dependent measurements of $LaCoO_3$ compound (25) have shown a gradual and weak change of the rhombohedral distortion, i.e., a gradual and a weak lattice expansion, both fine structure changes with temperature of the O and Co K-edges correspond to Co(3*d*, 4*p*)–O(2*p*) hybridization changes link to a spin-state transition which could result from dynamic structural modifications as it will be discussed later.

III.3. The Strontium Doping Effects at Oxygen K-Edges

The doping dependence of the O K-edge and of the prepeak region at O–K edges recorded at $T = 20$ K for the series $La_{1-x}Sr_xCoO_3$ ($x = 0$; 0.25; 0.5) is shown in Figs. 7a and 7b, respectively. The spectra correspond to transitions of unoccupied O 2*p* states mixed with Co 3*d* states as explained before. They are characteristic of hole-doped transition metal oxides and show the charge-transfer behavior of the Co–O bond in the $La_{1-x}Sr_xCoO_3$ system. Upon doping, the O–K edge prepeak shifts toward low energy and shows a drastic increase in intensity. Both indicate that new electronic states below the Fermi level are involved. They

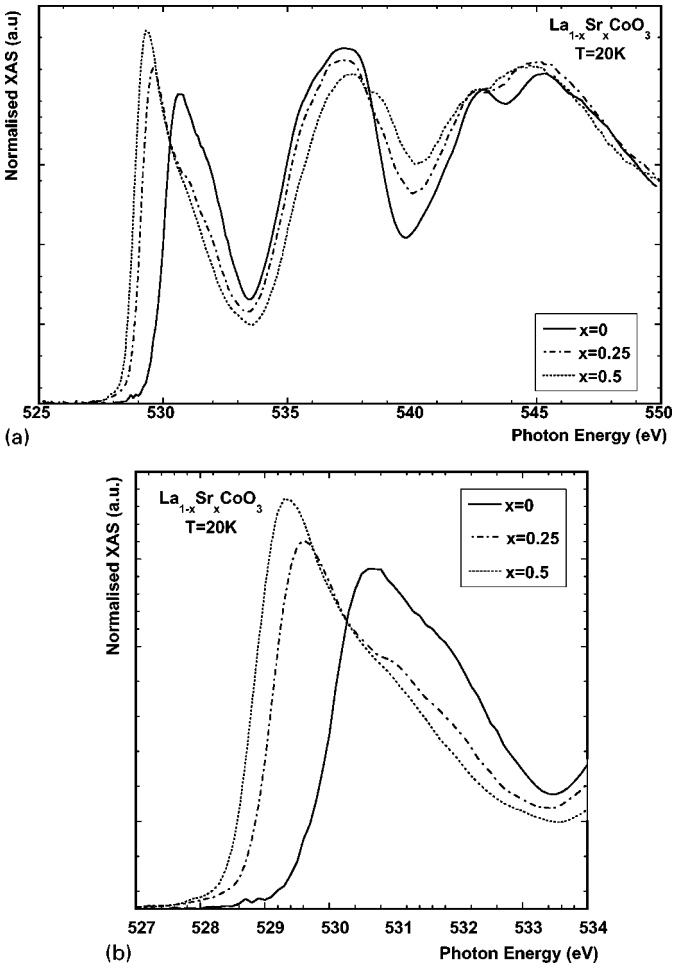

FIG. 7. Doping dependence at $T = 20$ K for the series $La_{1-x}Sr_xCoO_3$ ($x = 0$; 0.25; 0.5). (a) O K-edge; (b) O K-edge prepeak.

are due to the cobalt valence change expected upon doping and to the increase of the charge-transfer behavior. Note that such drastic doping changes were already observed in the transition metal series $La_{1-x}Sr_xMO_3$ (M = Fe and Mn) (26) and do agree with previous fluorescence yield measurements (27). Furthermore, the double peak structure observed on the higher energy part of the spectra between 540.5 and 550 eV, which is linked with hybridization between mixed Co 4*sp* and O 2*p* subbands, is deeply modified (Fig. 7a). This is again an indication of deep charge-transfer behavior change induced by strontium doping.

The temperature dependence of the two cobaltites $La_{1-x}Sr_xCoO_3$ ($x = 0.25$; 0.5) is shown in Figs. 8a and 8b, respectively. No drastic change with increasing temperature, i.e., neither through the gradual change in the metallic behavior around the Curie temperature nor through the ferromagnetic/paramagnetic transition, could be observed contrary to what was observed at the O K-edge in manganites through the metallic/semiconducting transition (28). Therefore, temperature variation does not induce a strong change in Co($3d, 4p$)–O($2p$) hybridization and, then, either in cobalt spin configuration and/or in Jahn–Teller distortion for the strontium-doped compounds in the probed temperature range.

III.4. Discussion

Let us consider first the double fine structure observed at 20 K on the prepeak of the O–K edge of $LaCoO_3$ compound. They should correspond to the e_g spin up and spin down subbands of LS Co^{3+}, respectively, as shown in the schematic energy level diagram of Fig. 9a. At low temperature, the nearly diamagnetic low state agrees with the magnetization measurements. On the derivative curve (Fig. 5c), the fine structure attributed to the e_g spin down subband of LS (t_{2g}^6) Co^{3+} (shoulder B′ at 531.5 eV) can be

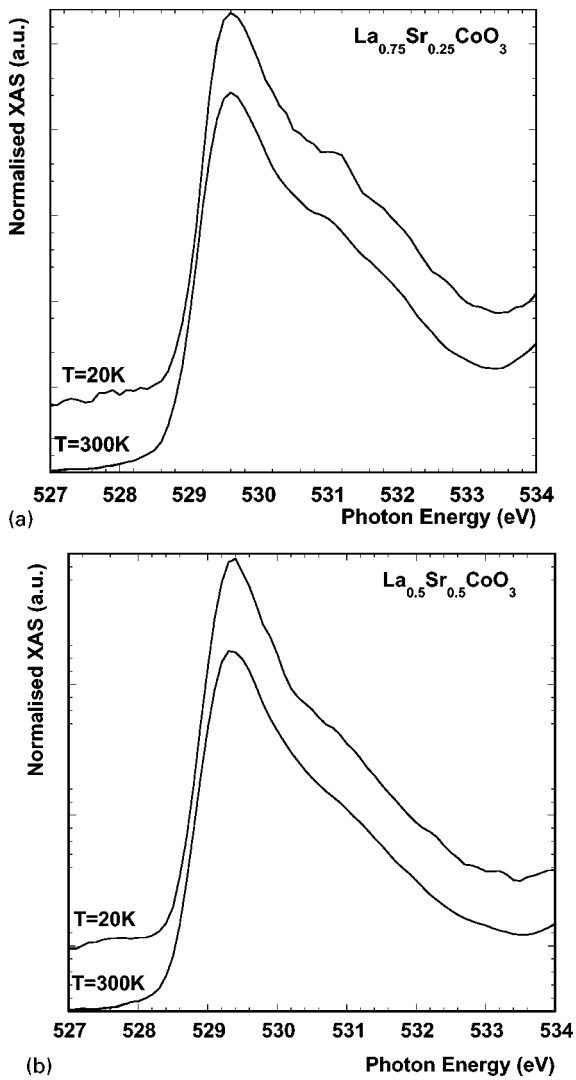

FIG. 8. O K-edge prepeak temperature dependence at $T = 20$ and 300 K: (a) $La_{0.75}Sr_{0.25}CoO_3$; (b) $La_{0.5}Sr_{0.5}CoO_3$.

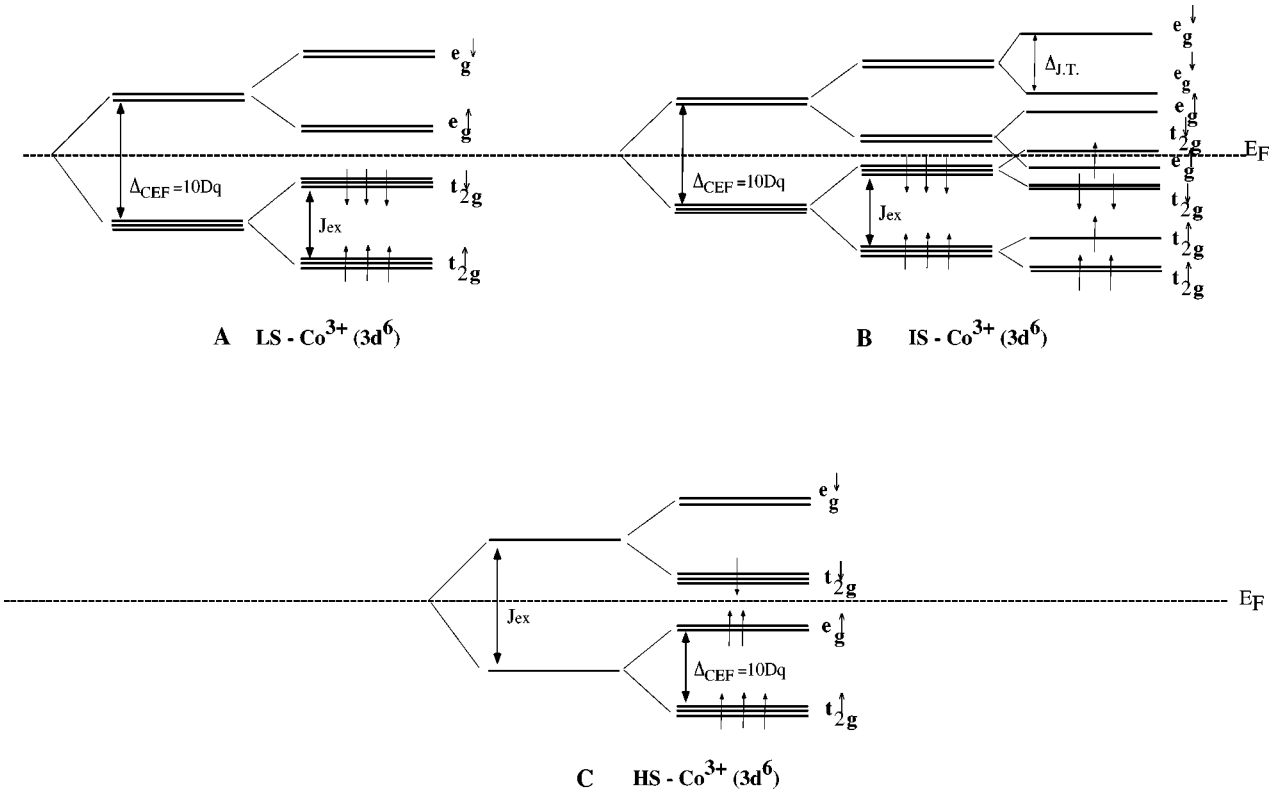

FIG. 9. Schematic diagram of the spin state of trivalent Co ions: (a) low spin, LS (t_{2g}^6) with $\Delta_{CEF} > J_{ex}$, where J_{ex} is the intraatomic exchange energy and Δ_{CEF} is the crystal field energy; (b) intermediate spin, IS ($t_{2g}^5 e_g^1$) with Jahn–Teller distortion; (c) high spin, HS ($t_{2g}^4 e_g^2$) with $\Delta_{CEF} < J_{ex}$.

resolved only at low temperature. At higher temperature, the fine structure seems mixed with other contributions. Assume that shoulder C′ at 529.4 eV corresponds to t_{2g} spin down IS ($t_{2g}^5 e_g^1$) Co^{3+} subband and that, at higher energy, shoulder A′ at 530 eV corresponds to e_g spin up LS (t_{2g}^6) Co^{3+} subband, then the continuous changes in intensity of shoulders A′ and C′ would reflect a continuous transition from LS Co^{3+} to *IS* Co^{3+} (Fig. 9b) upon heating. Let us label x_{LS} and x_{IS} as the spin populations in a low spin state and in an intermediate spin state, respectively. Therefore, the magnetic transition which occurs at $T = 110$ K could be interpreted as a change in the x_{LS}/x_{IS} ratio and as a paramagnetic ordering of the spin: at low temperature $x_{LS} > x_{IS}$, whereas above 110 K, $x_{LS} < x_{IS}$. In Fig. 5c, the both low spin A′ and intermediate spin C′ attributed fine structures are present whatever the temperature is. As mentioned before, the low spin state involves completely filled t_{2g} bands and then completely empty e_g states. Because the lobes of the t_{2g} orbitals point in between the oxygen ligand, whereas the lobes of the e_g orbitals point directly to the ligand, the overlap with O(2*p*) orbitals is greater for the e_g state. The spin transition from low spin to intermediate spin will then increase Co(3*d*)–O(2*p*) and Co(4*p*)–O(2*p*) hybridization as observed on the O and Co K-edges.

In Fig. 6, note that even if the experimental resolution does not permit us to clearly separate the two different contributions of the e_g spin up and down subband of LS (t_{2g}^6) Co^{3+} as it has been done at Fe K-edge (28), the pre-edge fine structure of the Co K-edge spectrum for Co^{3+} intermediate spin ($t_{2g}^5 e_g^1$) at room temperature is more diffuse than that from Co^{3+} low spin (t_{2g}^6) at low temperature as expected. Intermediate spin state involves a more hybridized state.

Considering the X-ray absorption characteristic time interaction (10^{-15}s), which is smaller than the typical phonon period in solids (10^{-13}s), it is the first time that such thermally active dynamic Jahn–Teller distortion is observed on cobaltites—the Co^{3+} low spin state is not a Jahn–Teller ion, whereas the Co^{3+} intermediate spin state is. This dynamic Jahn–Teller transition was suggested previously by Korotin *et al.* from band structure calculations (7). Moreover, the change in the x_{LS}/x_{IS} spin population ratio has also been suggested by Asai *et al.* (8) from their improvement of the mean-field theory model from Bari and Sivardiere (29) and by Radwanski *et al.* (30) from their low-energy electronic structure calculation. Our O K-edge observation of the low-spin to intermediate-spin smooth transition is in agreement with recent photoemission spectroscopy and magnetic

susceptibility data (10), with heat capacity measurements (31), and with infrared temperature-dependent spectroscopy (9).

When the temperature increases, the weak structural modification observed by neutron diffraction experiments (8, 11, 25) should induce a decrease of the crystal-field splitting and then contribute to the filling of the e_g spin up subband as illustrated in Fig. 9b. The IS Co^{3+} can then become metallic in agreement with LDA + U band structure calculations performed by Korotin *et al.* (7). Asai *et al.* (8) suggested the existence of a second spin-state transition near $T = 500$ K (from IS Co^{3+} to a mixed state of IS and HS Co^{3+} (Fig. 9c)) to explain the semiconducting to metal-like transition. This suggestion could be in agreement with previous O K- and Co $L_{2/3}$-edge measurements performed by Abbate (12), which showed the existence of a double peak structure at high temperature on the O–K absorption edges of $LaCoO_3$ compounds, which is interpreted as a signature of HS Co^{3+}. Let us consider our recent work at O–K edge on CMR manganese oxides (28), where a double peak structure on the O–K prepeak is shown in the metallic state correlated with a decrease of the dynamic Jahn–Teller distortion. The double-peak structure observed on the O–K edges of the $LaCoO_3$ compound above room temperature could then also be interpreted to be due to a decrease of the dynamic Jahn–Teller distortion with increasing temperature. This disappearance of the orbital ordering with increased temperature within the IS state has been suggested by Korotin *et al.* (7).

In summary, for $LaCoO_3$, a gradual transition from an LS to an IS state is observed with increasing temperature, which could account for the first magnetic transition to a paramagnetic state. The cobalt spin configuration at temperatures higher than 300 K is still controversial. The gradual metallic behavior, which occurs at high temperature, may be due either to a decrease of the crystal field splitting linked to a decrease of the dynamic Jahn–Teller distortion still within the IS state or to a second spin transition from IS Co^{3+} to a mixed state of IS and HS Co^{3+} or to complete HS Co^{3+}.

To understand the changes induced by strontium doping, one must first consider the previous X-ray magnetic circular dichroism (XMCD) measurements at O K-edge performed by Pellegrin (32), which showed a negative asymmetry on the unoccupied O 2p mixed with cobalt 3d states. This negative asymmetry has recently been confirmed by Okamoto *et al.* (33). Following the same framework used to interpret XMCD measurements at O K-edge in manganites (28), the negative fine structure observed in cobaltites is compatible with the presence of states with spin down symmetries just above the Fermi level, then with LS (t_{2g}^5) Co^{4+} or IS $(t_{2g}^4 e_g^1)$ Co^{4+}. Consider now the first-principles full-potential calculations indicating that the formal Co^{4+} charge in the $La_{1-x}Sr_xCoO_3$ system should be closer to an IS configuration rather than to a LS configuration (34), we assume that the new electronic states below the Fermi level induced by strontium doping are likely due to the presence of IS $(t_{2g}^4 e_g^1)$ Co^{4+}. This electronic configuration could be seen as a HS Co^{3+} $(t_{2g}^4 e_g^2)$ configuration antiferromagnetically coupled to O 2p ligand holes in a way similar to the one proposed by the ZSA model (35). Then, strontium doping should also induce a partial spin-state transition from LS Co^{3+} (in the undoped compound) to HS Co^{3+} configuration antiferromagnetically coupled to O 2p ligand holes. From an experimental point of view, this intermediate state has also been suggested by Okamoto *et al.* (33) to interpret their Co 2p and O 1s XMCD data. Previous Co 2p XAS and atomic mutiplet calculation work performed by Potze *et al.* (36) on $SrCoO_3$ compounds also detected the presence of IS Co^{4+}.

Nevertheless, if we consider the mixed valence state expected, our measurements do not allow us to distinguish between LS and IS for Co^{3+} electronic configurations. Taking into account that an increase of the cobalt formal charge, when going from $x = 0$ to $x = 0.5$ strontium doping, should decrease the ionic radius thus the Co–O distances; one could expect it to lower the spin state. However, neutron diffraction measurements showed an increase of the Co–O distances (11, 15) by strontium doping at low temperature ($T = 20$ K). The authors suggested that the increase of the ionic radius is likely due to an increase of the cobalt spin configuration when going from a low spin to a higher spin state (1.89 Å for LS Co^{3+} and 1.95 Å for HS Co^{3+} (37)). From our O 1s measurements, we also suggest a mixed LS–IS Co^{3+}/IS Co^{4+} cobalt ion configuration at low temperature. Futhermore, because of our O K-edge temperature dependance, which does not show any drastic changes, we also suggest the presence of an admixture of LS and IS Co^{3+} electronic configurations at room temperature, which agrees with photoemission Sr doping dependence spectroscopy (38).

It should be noted that the large observed magnetostriction at low temperature (20) cannot arise from LS Co^{3+} but could be then due to a spin transition from LS Co^{3+} to IS Co^{3+} induced by the applied magnetic field. Therefore, even if localized-electron and itinerant-electron phase segregation and double exchange interactions are observed in both manganites (39) and cobaltites systems (15), the fundamental mechanism governing the magnetotransport properties seem different. Manganites show lower magnetostriction effects (40). In the cobaltites, the small magneto-transport effect seems to be due mainly to the growth of ferromagnetic clusters as suggested by the magnetization measurements (also observed on manganites) and to a spin transition from LS Co^{3+} to IS Co^{3+} under an applied magnetic field, whereas, in manganites, the loss of the electron–phonon interaction plays a key role at the semiconducting/metal-like transition (28, 41). One could

suggest here that magnetic phase separation might be intrinsic in the perovskite systems, since the observation of similar stripe fluctuations in Sr-doped cuprates and oxygen-doped nickelates (42)—not directly responsible for colossal magneto-transport effect.

IV. CONCLUSION

High-resolution soft X-ray absorption spectroscopy at O K-edge of cobalt oxides was performed at NSLS (BNL, Brookhaven) in fluorescence mode. Strontium doping and thermal dependence of $LaCoO_3$ were realized, allowing us to perform an analysis of the pre-edge fine structures in the assumption that this pre-edge corresponds to Co 3*d* subbands due to hybridization of Co(3*d*) and O(2*p*) electronic levels. This is new evidence that high-resolution soft X-ray absorption spectroscopy at O K-edge can give information about the spin configurations of transition metal in oxides.

More precisely, the thermal dependence of the prepeak at the O K-edge for $LaCoO_3$ brought new evidence for a continuous smooth spin transition from a low spin to an intermediate spin Co^{3+} considering the X-ray absorption characteristic time interaction (10^{-15}s), which is smaller than the typical phonon period in solids (10^{-13}s).

Upon strontium doping of $LaCoO_3$, the observed changes in the prepeak fine structure at O K-edge suggested that a mixed LS–IS Co^{3+}/IS Co^{4+} cobalt ion configuration occurs. The IS Co^{4+} electronic configuration must be seen as a HS Co^{3+} configuration antiferromagnetically coupled to O 2*p* ligand holes. Our temperature dependence measurements at the O K-edge for the compounds $La_{1-x}Sr_xCoO_3$ ($x = 0.25; 0.5$) do not show any drastic change through the gradual change in the metalic behavior around the Curie temperature, which is contrary to what was observed at the O K-edge in manganites. Therefore, even if phase segregation was observed in manganites and in cobaltite perovskite systems, the fundamental mechanism governing the magnetotransport properties seem different in both systems.

ACKNOWLEDGMENT

We are grateful to J. H. Park of the NSLS in Brookhaven for his help and advice during the X-ray absorption experiment.

REFERENCES

1. R. M. Kuster, J. Singleton, D. A. Keon, R. M. Greedy, and W. Hayes, *Physica B* **155,** 362 (1989); R. Von Hemmolt, J. Wecker, B. Holzapfel, L. Schultz, and K. Samwer, *Phys. Rev. Lett.* **71,** 2331 (1993); H. L. Ju, C. Kwon, Q. Li, R. L. Greene, and T. Venkaten, *Appl. Phys. Lett.* **65,** 2108 (1994); A. Maignan, Ch. Simon, V. Caignaert, and B. Raveau, *Solid State Commun.* **96,** 623 (1995); R. Mahesh, R. Mahendiran, A. K. Raychaudhury, and C. N. R. Rao, *J. Solid State Chem.* **114,** 297 (1995); S. Jin, H. M. O'Bryan, T. H. Tiefel, M. McCormack, and W. W. Rhodes, *Appl. Phys. Lett.* **66,** 382 (1995).
2. B. Raveau, A. Maignan, and C. Martin, *J. Solid State Chem.* **130,** 162 (1997); A. Maignan, F. Damay, C. Martin, and B. Raveau, *Mater. Res. Bull.* **32,** 965 (1997).
3. G. Briceno, H. Chang, X. Sun, P. G. Schultz, and X. D. Xiang, *Science* **270,** 273 (1995); S. Yamaguchi, H. Taniguchi, H. Takagi, T. Arima, and Y. Tokura, *J. Phys. Soc. Jpn.* **64,** 1885 (1995); R. Mahendiran, A. K. Raychaudhui, A. Chainani, and D. D. Sarma, *J. Phys. Condens. Matter* **7,** L561 (1995); V. Golovanov, L. Mihaly, and A. R. Moodenbaugh, *Phys. Rev. B* **53,** 13, 8207 (1996).
4. J. Perez, J. Garcia, J. Blasco, and J. Stankiewicz, *Phys. Rev. Lett.* **80,** 11, 2401 (1998).
5. K. I. Kobayashi, T. Kimura, H. Sawada, K. Terakura, and Y. Tokura, *Nature* **395,** 677 (1998).
6. C. S. Naiman, R. Gilmore, B. DiBatolo, A. Linz, and R. Santoro, *J. Appl. Phys.* **36,** 1044 (1965).
7. M. A. Korotin, S. Yu Ezhov, I. V. Solovyev, V. I. Anisimov, D. I. Komskii, and G. A. Sawatzky, *Phys. Rev. B* **54**(8), 5309 (1996).
8. K. Asai, A. Yoneda, O. Yokokura, J. M. Tranquada, G. Shirane, and K. Kohn, *J. of the Phys. Soc. Jpn.* **67**(1), 290 (1998).
9. S. Yamaguchi, Y. Okimoto, and T. Tokura, *Phys. Rev. B* **55**(14), R8666 (1997).
10. T. Saitoh, T. Mizokawa, A. Fujimori, M. Abbate, Y. Takeda, and M. Takano, *Phys. Rev. B* **55**(7), 4257 (1997).
11. D. Louca, J. L. Sarrao, J. D. Thompson, H. Roder, and G. H. Kwei, *Phys. Rev. B* **60,** 10,378 (1999).
12. M. Abbate, J. C. Fugle, A. Fujimori, L. H. Tjeng, C. T. Chen, R. Potze, G. A. Sawatski, H. Eisaki, and S. Uchida, *Phys. Rev. B* **47**(24), 16,124 (1993).
13. M. A. Senaris-Rodriguez and J. B. Goodenough, *J. Solid State Chem.* **118,** 323 (1995).
14. S. Yamaguchi, Y. Okimoto, H. Taniguchi, and Y. Tokura, *Phys. Rev. B* **53,** R2926 (1996).
15. R. Caciuffo, D. Rinaldi, G. Barucca, J. Mira, J. Rivas, M. A. Senaris-Rodriguez, P. G. Radaelli, D. Fiorani, and J. B. Goodenough, *Phys. Rev. B* **59**(2), 1068 (1999).
16. M. Itoh, I. Natori, S. Kubato, and K. Mototya, *J. Phys. Soc. Jpn.* **63**(4), 1486 (1994).
17. W. C. Koehler and E. O. Wollan, *J. Phys. Chem. Solids* **2,** 100 (1957).
18. O. Toulemonde, F. Studer, A. Llobet, L. Ranno, A. Maignan, E. Pollert, M. Nevriva, E. Pellegrin, N. B. Brooks, and J. B. Goedkoop, *J. Magn. Magn. Mater* **190,** 307 (1998).
19. J. M. De Teresa, M. R. Ibarra, P. A. Algarabel, C. Ritter, C. Marquina, J. Blasco, J. Garcia, A. del Moral, and Z. Arnold, *Nature* **386,** 256 (1997).
20. M. R. Ibarra, R. Mahendiran, C. Marquina, B. Garcia-Landa, and J. Blasco, *Phys. Rev. B* **57**(6), R3217 (1998).
21. C. Zener, *Phys. Rev.* **82,** 403 (1951); P. W. Anderson and H. Hasegawa, *Phys. Rev.* **100,** 975 (1955); P. G. De Gennes, *Phys. Rev.* **118,** 141 (1960).
22. F. M. F. de Groot, M. Grioni, J. C. Fuggle, J. Ghijsen, G. A. Sawatzky, and H. Petersen, *Phys. Rev. B* **40**(8), 5715 (1989).
23. M. Croft, D. Sills, M. Greenblatt, C. Lee, S. W. Cheong, K. V. Ramanujachary, and D. Tran, *Phys. Rev. B* **55,** 8726 (1997).
24. G. Thornton, I. W. Owen, and G. P. Diakun, *J. Phys. Condens. Matter* **3,** 417 (1991).
25. G. Thornton, B. C. Tofield, and A. H. Hewat, *J. Solid State Chem.* **61,** 301 (1986).
26. M. Abbate, F. M. M. De Groot, J. C. Fuggle, A. Fjmori. O. Strebel, F. Lopez, M. Domke, G. Kaindl, G. A. Sawatsky, M. Takano, Y. Takeda, H. Eisaka, and S. Uchiba, *Phys. Rev. B* **46,** 4511 (1992).
27. A. R. Moodenbaugh, B. Nielsen, S. Sambasivan, D. A. Fischer, T. Friessnegg, S. Aggarwal, R. Ramesh, and R. L. Pfeffer, *Phys. Rev. B* **61,** 5666 (2000).
28. O. Toulemonde, F. Millange, F. Studer, B. Raveau, J. H. Park, and C. T. Chen, *J. Phys. Condens. Matter* **11,** 109 (1999).

29. R. A. Bari and J. Sivardiere, *Phys. Rev. B* **5,** 4466 (1972).
30. R. J. Radwanski and Z. Ropka, *Physica B* **281&282,** 507 (2000).
31. S. Stolen, F. Gronvold, H. Brinks, T. Atake, and H. Mori, *Phys. Rev. B* **55**(21), 14,103 (1997).
32. E. Pellegrin, G. A. Sawatsky, M. H. R. Lankhorst, H. J. M. Bouwmeester, H. Verweij, R. Van den Oetelaar, and C. F. J. Flipse, ESRF Report, 1997.
33. J. Okamoto, H. Miyauchi, T. Sekine, T. Shidara, T. Koide, K. Amemiya, A. Fujimori, T. Saitoh, A. Tanaka, Y. Takeda, and M. Takano, *Phys. Rev. B* **62,** 4455 (2000).
34. P. Ravindran, P. A. Korzhavyi, H. Fjellvag, and A. Kjekshus, *Phys. Rev. B* **60,** 16423 (1999).
35. J. Zaanen, G. A. Sawatsky, and J. W. Allen, *Phys. Rev. Lett.* **55,** 418 (1985).
36. R. H. Potze, G. A. Sawatzky, and M. Abbate, *Phys. Rev. B* **51**(17), 11,501 (1995).
37. R. D. Shannon, *Acta Crystallogr. Sect. A* **32,** 751 (1976).
38. T. Saitoh, T. Mizokawa, A. Fujimori, M. Abbate, Y. Takeda, and M. Takano, *Phys. Rev. B* **56**(3), 1290 (1997).
39. G. Allodi, R. De Renzi, G. Guidi, F. Licci, and M. W. Pieper, *Phys. Rev. B* **56,** 6036 (1997); M. Uehara, S. Mori, C. H. Chen, and S. W. Cheong, *Nature* **399,** 560 (1999); Y. Moritomo, A. Machida, S. Mori, N. Yamamoto, and A. Nakamura, *Phys. Rev. B* **60,** 9220 (1999); C. Ritter, R. Mahendiran, M. R. Ibarra, L. Morellon, A. Maignan, B. Raveau, and C. N. R. Rao, *Phys. Rev. B* **61,** R9229 (2000).
40. J. M. De Teresa, M. R. Ibarra, J. Blasco, J. Garcia, C. Mrquina, P. A. Algrabel, Z. Arnold, K. Kamenev, C. Ritter, and R. Von Helmolt, *Phys. Rev. B* **54,** 1197 (1996).
41. A. J. Millis, P. B. Litlewood, and B. I. Shraiman, *Phys. Rev. Lett.* **74,** 5144 (1995); A. J. Millis, B. I. Shraiman, and R. Mueller, *Phys. Rev. Lett.* **77,** 175 (1996).
42. I. M. Abu-Shiekah, O. O. Bernal, A. A. Menovsky, H. B. Brom, and J. Zaanen, *Phys. Rev. Lett.* **83,** 3309 (1999).